

Aberystwyth University

Jupiter's polar ionospheric flows

Johnson, Rosie E.; Stallard, Tom S.; Melin, Henrik; Nichols, Jonathan D.; Cowley, Stan W.H.

Published in:

Journal of Geophysical Research: Space Physics

DOI:

[10.1002/2017JA024176](https://doi.org/10.1002/2017JA024176)

Publication date:

2017

Citation for published version (APA):

Johnson, R. E., Stallard, T. S., Melin, H., Nichols, J. D., & Cowley, S. W. H. (2017). Jupiter's polar ionospheric flows: High resolution mapping of spectral intensity and line-of-sight velocity of H³⁺ ions. *Journal of Geophysical Research: Space Physics*, 122(7), 7599-7618. <https://doi.org/10.1002/2017JA024176>

Document License

CC BY

General rights

Copyright and moral rights for the publications made accessible in the Aberystwyth Research Portal (the Institutional Repository) are retained by the authors and/or other copyright owners and it is a condition of accessing publications that users recognise and abide by the legal requirements associated with these rights.

- Users may download and print one copy of any publication from the Aberystwyth Research Portal for the purpose of private study or research.
- You may not further distribute the material or use it for any profit-making activity or commercial gain
- You may freely distribute the URL identifying the publication in the Aberystwyth Research Portal

Take down policy

If you believe that this document breaches copyright please contact us providing details, and we will remove access to the work immediately and investigate your claim.

tel: +44 1970 62 2400
email: is@aber.ac.uk

JGR: Space Physics

Supporting Information for

Jupiter's polar ionospheric flows: High resolution mapping of spectral intensity and line-of-sight velocity of H_3^+ ions

Rosie E. Johnson^{1*}, Tom S. Stallard¹, Henrik Melin¹, Jonathan D. Nichols¹
and Stan W. H. Cowley¹

(1) Department of Physics and Astronomy, University of Leicester, Leicester, UK

* Corresponding author:

Rosie Johnson

Department of Physics and Astronomy

University of Leicester

University Road

Leicester LE1 7RH, U.K.

E-mail address: rej17@le.ac.uk

Telephone: [+44\(0\)116 252 1302](tel:+44(0)116 252 1302)

Contents of this file

Fitting the H_3^+ emission line S1

Limb Fitting S2

Line-of-sight intensity correction S3

Spatial Correction S4

Errors S5

Introduction

This supporting information outlines in greater detail the methods described in the main paper the associated uncertainties accumulating during the data analysis process.

Fitting the H_3^+ emission line S1

An example of fitting the Gaussian profile (Equation 6) to the intensity at a spatial row position along the average H_3^+ emission line is shown in Figure S1 as the red line; similar fits were produced for each spatial position.

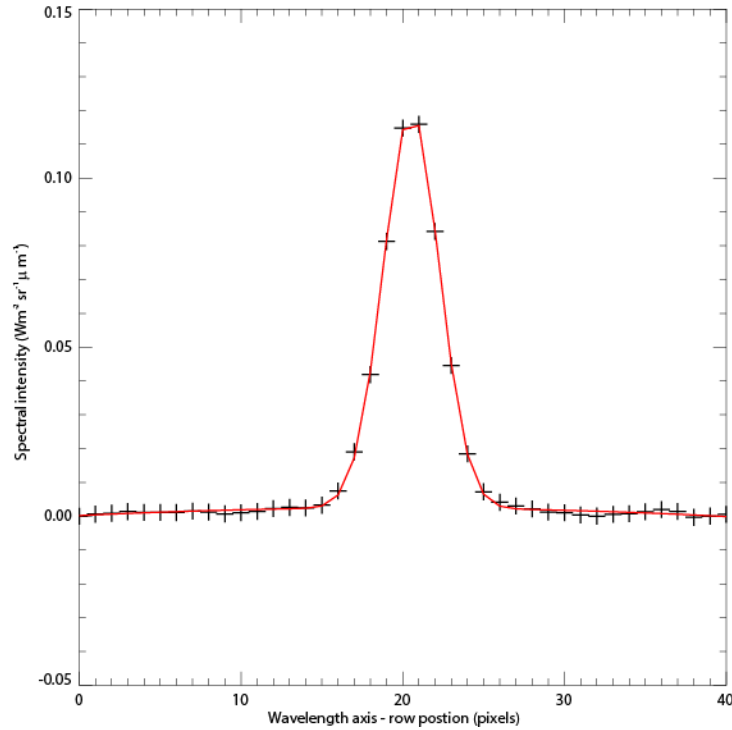


Figure S1 – An example of a Gaussian profile superposed on a slowly-varying quadratic background fitted to a spatial row position along the average H_3^+ emission line. This Gaussian was fitted to the 350th spatial position along the slit length. The slit was positioned at latitude $\sim 66^\circ$ and CML $\sim 173^\circ$. The intensity is represented by the crosses and the fitted Gaussian is represented by the red line.

Limb Fitting S2

It is essential at this stage of the data analysis to locate the limbs of the planet on the spectral image in order to perform further corrections. On the 31 December 2012, Jupiter's equatorial diameter subtended $46.92''$ in the sky. The slit length of CRIRES is $40''$ therefore the slit encompasses both limbs in the auroral regions. By sequentially plotting the spectral intensity derived for each slit position, a spectral intensity map of Jupiter's northern aurora is created and is shown in Figure S2. This spectral image is identical to the spectral image which has been mapped onto a polar projection in Figure 1, and therefore the same regions of morphology are identifiable. The H_3^+ emission on the disk and the higher intensity of emission in the auroral regions can be observed. As no H_3^+ ions exist outside of Jupiter's atmosphere, measurements recorded off the disk are assumed to be caused by noise. In Figure S2, the emission observed on the dawn limb is weaker than the emission observed on the dusk limb. Since the dawn

limb is not fully illuminated, and production rates of H_3^+ are not instantaneous, the production rates of H_3^+ are lower than at the dusk limb.

To locate the limbs the spectral image was overlaid with a calculated planetary limb, accounting for Jupiter's polar flattening, the sub-Earth latitude, and the plate scale of CRITES. The planetary limb was calculated from an oblate spheroid which has a semi-major axis of Jupiter's equatorial radius and a semi-minor axis of Jupiter's polar radius at the 1 bar level, both radii with an additional 550 km altitude to approximate the peak emission height of H_3^+ (Melin et al., 2005). The position of the calculated planetary limb (blue dashed line) was manually fitted to the dusk limb of the planet, as this limb was fully illuminated. It was assumed that there was no drifting of the telescope during a scan and the guiding was completely accurate. This is a reasonable assumption due to the reliable off-axis guiding provided by the VLT.

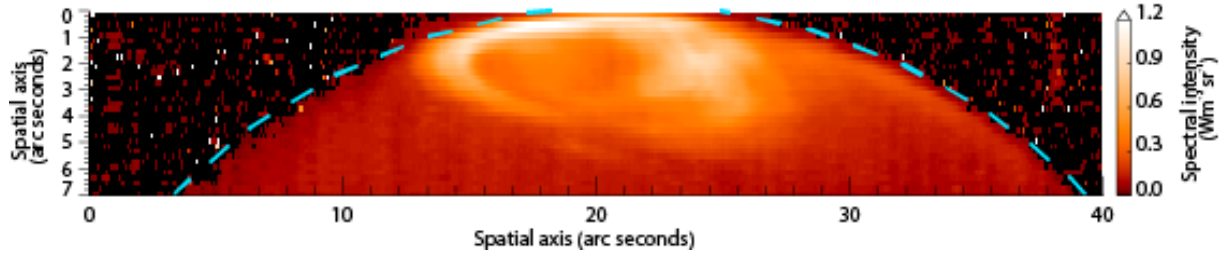


Figure S2 – A spectral image covering a CML range of $180^\circ - 193^\circ$, overlaid with a calculated planetary limb (blue dashed line) which was manually fitted to the planetary disk. A gamma correction of 0.2 was applied to the spectral image. The x-axis corresponds to the slit width ($40''$) and the y-axis corresponds to the scan length. Each step in the scan is equivalent to one slit width ($0.2''$) and the total scan length is $\sim 7''$ which was 36 steps (note that Jupiter's equatorial width during the observations was $\sim 47''$).

Line-of-sight intensity correction S3

The LOS correction is performed on the spectral intensity by calculating the limb brightening and removing this from the spectral images. The pathway from the centre of the planet to each pixel (r_{pathway}) can then be determined. The LOS correction value (LOS_c) is determined using a cosine function of the pathway (r_{pathway}) and the planetary radius ($r_{\text{planetary_radius}}$) at the particular latitude of the pixel.

$$LOS_c = \cos\left(\frac{r_{\text{pathway}}}{r_{\text{planetary_radius}}}\right)$$

Equation S1

The LOS correction calculated for an individual spectral line is shown as the dashed red line in Figure S3. The uncorrected spectral intensity is shown as the black dotted line in Figure S3. The LOS correction is performed through multiplication of the LOS correction values and the uncorrected spectral intensity values.

$$I_{LOS_c} = I \times LOS_c$$

Equation S2

The correction reduces the spectral intensity across the whole region (as the entire auroral region is located close to the limb), with the limb brightening effect strongest at the ends of the slit. After correction, the LOS corrected spectral intensity (I_{LOS_c}) is significantly lower, as shown by the black line.

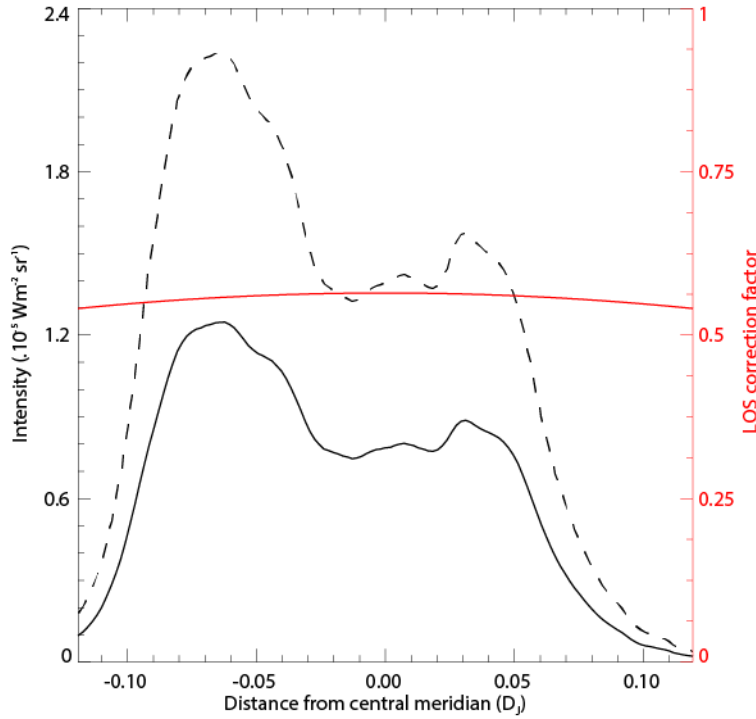


Figure S3 – Spectral intensity taken at CML $\sim 170^\circ$ and latitude of $\sim 82^\circ$. The dashed red line represents the LOS correction factor that is applied to the reduced data. The black dashed line represents the spectral intensity derived prior to LOS corrections. The black line represents the spectral intensity after the LOS correction is performed.

Figure S4a shows the spectral intensity at CML $\sim 180^\circ$ mapped onto a polar projection before LOS intensity correction, where spectral intensity towards the limb of Jupiter appears brighter than it actually is. Figure 15b shows the spectral intensity at CML $\sim 180^\circ$ mapped onto a polar projection after LOS intensity correction. When comparing the Figure S4a and Figure S4b, it can be seen that the spectral intensity at the limbs has been reduced and Figure S4b is a more accurate representation of the actual H_3^+ emission.

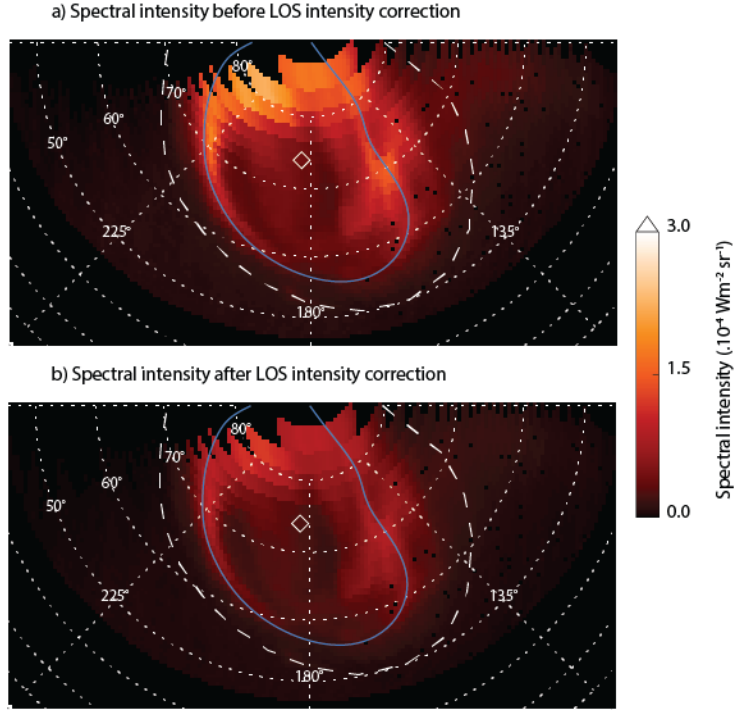


Figure S4 – Polar projections of spectral intensity (a) before and (b) after the line-of-sight (LOS) intensity correction was performed. A gamma correction of 0.6 was applied to the projected spectral images in both (a) and (b).

Spatial Correction S4

By using near-simultaneous images of the H_3^+ emission, Stallard et al. (2001) could determine the per pixel variation of spectral intensity inside the slit. There are no H_3^+ images available for the CRIRES data set, and therefore the spectral intensity variation inside the slit must be approximated by interpolating between slit positions. Figure S5 shows a schematic of intensity anisotropies that can occur inside the slit. A pixel of interest is chosen on the limb of the planet, which is bound by the blue box. The spectral intensity at three positions inside the slit (P_1 , P_2 and P_3) are determined by interpolating across the three slit positions (S_1 , S_2 and S_3) shown in Figure S5. In the enlargement of the pixel of interest in Figure S5, it can be seen that the intensity variation across the slit is not constant. When fitting a Gaussian to the intensity inside this pixel of interest the peak is shifted towards P_1 , which causes additional wavelength shifts on top of any existing Doppler shift due to the motion of the H_3^+ ions. The spectral intensity variation $\Delta I(x, y)$ in the pixel of interest can be modelled,

$$I(x, y) = \frac{p_3 - p_1}{p_3 + p_1}$$

Equation S3

where p_1 is the pixel at the bottom of the slit and p_3 is the pixel at the top of the slit, as shown in Figure S5.

The spectral intensity variation is related to the spatial velocity Δv_s through a linear relationship with a constant b ,

$$\Delta v_s(y) = b \Delta I(x, y).$$

Equation S4

Stallard et al. (2001) determined the constant b value theoretically and empirically. The theoretical velocity resolution of the 0.5'' slit of the IRTF instrument, CSHELL, is 7 km s⁻¹. Through testing this value against others, Stallard et al. (2001) empirically determined the b value to be 10 km s⁻¹, by using simulated illumination calculated from the H₃⁺ images. The theoretical velocity resolution for the 0.2'' CRIRES slit is 3 km s⁻¹, and this value was tested empirically on the CRIRES data and was found to be a suitable value for the constant b . It should be noted that since the emission line spreads across several pixels, by using a Gaussian to fit the emission line to sub-pixel accuracy, LOS velocity values smaller than the theoretical velocity resolution may be derived. Stallard et al. (2001) estimated a Gaussian could be fitted to the position of the emission line to an accuracy of 0.1 pixels, suggesting the Gaussian fitting accuracy in this paper is ~300 m s⁻¹.

Once the spatial velocity, Δv_s , was determined for each pixel this value could be removed from the derived LOS velocity in the appropriate reference frame, as shown in the equations below.

$$v_{MPRF_{sc}}(y) = v_{MPRF}(y) - \Delta v_s(y),$$

Equation S5

and

$$v_{PRF_{sc}}(y) = v_{PRF}(y) - \Delta v_s(y).$$

Equation S6

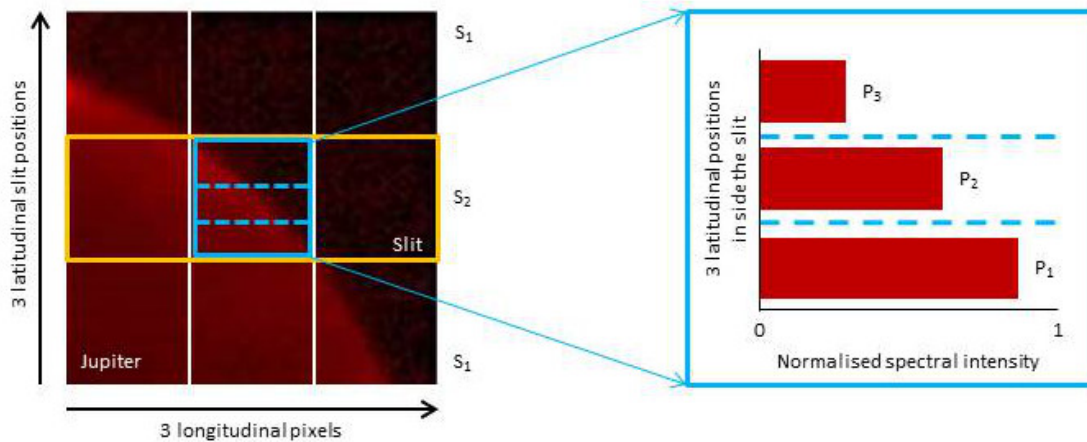


Figure S5 – A schematic showing the intensity anisotropies which occur inside the slit. The slit width is exaggerated to emphasize the anisotropies inside the slit. The blue box bounds the pixel of interest, and the intensity values inside the pixel were determined through interpolation of the intensity inside the slit across three slit positions (S_1 , S_2 and S_3). Once the intensity inside the slit is known the intensity variation inside the slit can be determined, from which the spatial velocity can be derived.

shows a comparison of the LOS velocity in the PRF before and after spatial correction was applied, when the center of the slit was positioned at $\sim 74^\circ$ latitude. The spatial velocities, derived from the intensity anisotropies, are represented in by the black line. The spectral intensity is represented in by the grey dotted line. The spatial velocity varies as the spectral intensity varies; in particular large spatial velocities are derived at the limb due to the significant intensity gradient here. The green crosses are the LOS velocity in the PRF before spatial correction is performed. It can be seen that the majority of the variation is independent of the spatial velocities (black line). This implies that the LOS velocity in the PRF is derived from Doppler shift caused by the H_3^+ motions, with only small additional Doppler shifts caused by the spatial effects. As CRIRES has a narrow slit of $0.2''$ there is less spatial variation across the slit width, which acts to reduction the spatial effects compared to the study by Stallard et al. (2001).

Towards the limb, beyond $\sim -0.16 D_J$ and $\sim 0.16 D_J$, however, the positive values in the LOS velocity (green dashed line) are caused by the spatial anisotropies creating additional blue-shifts in the spatial velocity (black line). By removing the spatial velocity as in Equation S6, the blue-shift on the limb can be reduced. In this sub-auroral dusk region of Jupiter's ionosphere, we would expect the ions to be corotating and hence derive a LOS velocity of $\sim 0 \text{ km s}^{-1}$ in the PRF. The pink crosses show the LOS velocities in the PRF after spatial correction. At $\sim 0.16 R_J$ it can be seen that the blue-shifted velocities are significantly reduced to $\sim 0 \text{ km s}^{-1}$ after the spatial correction is performed. A similar reduction is also seen on the dawn limb at $\sim -0.16 R_J$, however unreliable results are seen at distances larger than $\sim -0.17 R_J$, due to a greater level of noise on the dawn limb compared to the dusk limb, as discussed previously in section 4.2. There is some variation seen across the main auroral emission and polar aurora, however the values differ significantly from the derived LOS velocity in the PRF unlike towards the limb

where the values of spatial velocity are very similar to the derived LOS velocity in the PRF.

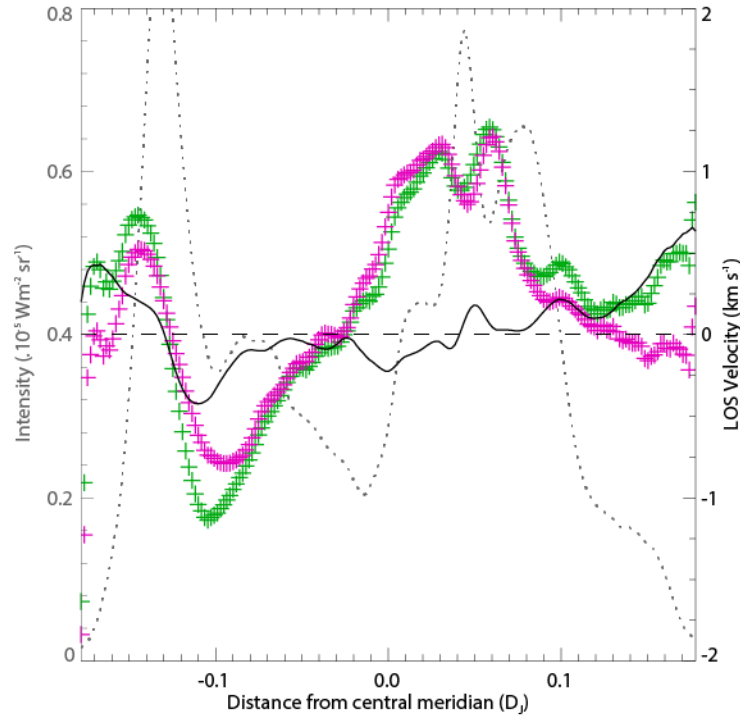


Figure S6 – A comparison of the LOS velocity before and after spatial correction in the planetary reference frame (PRF), when the center of the slit was positioned at CML $\sim 171^\circ$ and latitude $\sim 74^\circ$. The spectral intensity is represented by the grey dotted line. The spatial velocities, calculated using Equation S4, are represented by the black line. The LOS velocity before correction, $v_{\text{PRF}}(y)$, is represented by the green crosses and the LOS velocity after correction, $v_{\text{PRF}_{sc}}(y)$, is represented by the pink crosses. The black dashed line of zero gradient represents corotation in the PRF.

Errors S5

Projection S5.1

As with all projections, there are large errors associated with the pixels that map toward the planetary limb. Pixels located at the limb will map to a larger range of latitudes and longitudes than pixels located at the centre of planet. In addition, pixels at the limb at higher latitudes map to a larger range of latitudes and longitudes than pixels located at the limb at lower latitudes. For example, at the most equatorial slit position ($\sim 45^\circ$ latitude), a pixel at the limb covers a longitude range of $\sim 2.2^\circ$ and a latitude range of $\sim 0.7^\circ$. However, at the most poleward slit position ($\sim 86^\circ$ latitude), a pixel at the limb covers a longitude range of $\sim 4.1^\circ$ and a latitude range of $\sim 2.6^\circ$.

The polar projections are created from a series of spectra measured over 25 seconds. During this time Jupiter will rotate 0.26° causing a smearing of 0.504 pixels in the spectra in the spatial direction. However, this smearing is smaller than the seeing ($\sim 0.5''$, which equates to ~ 5.6 pixels) and hence is not a significant error.

Despite the errors in creating the projections, the precise mapping of the flows is not the main aim of this study. Although the errors must be noted, the positional discrepancies do not affect the main results of this investigation. By creating polar projections of the spectral images and ion flows using the same method, the spectral intensity morphology can still be directly compared with the flow regimes. However, if one were to consider how the flow regions in Jupiter's ionosphere map to the magnetosphere then it would be wise to use caution.

Spectral dispersion S5.2

As explained in Appendix A4, the wavelength variation across the detector array was determined using the telluric emission lines, which was part of the data reduction. During this process the 1-sigma error estimate on the position of the peak of Gaussian fitted to every spatial position along the telluric emission line and the 1-sigma error estimate on the second order polynomial which was fitted to the telluric emission line were determined. The total error from correcting the spectral dispersion was 0.053 km s^{-1} , which includes the uncertainties from fitting a Gaussian and from fitting a second order polynomial to the telluric emission line.

Fitting a Gaussian S5.3

To derive the LOS velocities from the H_3^+ emission line the exact position of the line must be known so the relative Doppler shift can be related to the resolution of the instrument. By fitting a Gaussian to every spatial position along the average H_3^+ emission line, the position of the Gaussian was identified and hence the relative Doppler shift was determined. Therefore associated with each derived value of LOS velocity there is a 1-sigma error on fitting this Gaussian.

v_0 S5.4

The value v_0 was determined by fitting a Gaussian to the equatorial region of the average spectra taken in a North-South orientation. There is an uncertainty associated with the position of the peak of this Gaussian which is included in the v_0 uncertainty. The accuracy of aligning the slit with the centre of the planet was $\sim \pm 1''$ in the longitudinal direction, which introduces a small LOS velocity values due to the rotation of the planet. Both of these uncertainties are taken into account and a final uncertainty of $\pm 0.15 \text{ km s}^{-1}$ is applied to all measured LOS velocities values in all reference frames.

Spatial correction S5.5

Performing the spatial correction on the LOS velocity values introduces uncertainties because no simultaneous H_3^+ images were available to determine the spectral intensity variation inside the slit, and therefore the calculated spatial velocities are an approximation. The 1-sigma error from fitting a 2D polynomial to the interpolated results is included in the total error for each derived value of LOS velocity.